From the triangular to the kagome lattice: Following the footprints of the ordered state

Liliana Arrachea,[1,2,*] Luca Capriotti,[3] and Sandro Sorella[1]
[1]*International School for Advanced Studies (SISSA) and INFM-Democritos, National Simulation Centre, I-34014 Trieste, Italy*
[2]*Max Planck Institut für Physik komplexer Systeme, Dresden, Germany*
[3]*Kavli Institute for Theoretical Physics, University of California, Santa Barbara, California 93106-4030, USA*
(Received 24 November 2003; revised manuscript received 24 March 2004; published 29 June 2004)

We study the spin-1/2 Heisenberg model in a lattice that interpolates between the triangular and the kagome lattices. The exchange interaction along the bonds of the kagome lattice is J, and the one along the bonds connecting kagome and nonkagome sites is J', so that $J'=J$ corresponds to the triangular limit and $J'=0$ to the kagome one. We use variational and exact diagonalization techniques. We analyze the behavior of the order parameter for the antiferromagnetic phase of the triangular lattice, the spin gap, and the structure of the spin excitations as functions of J'/J. Our results indicate that the antiferromagnetic order is not affected by the reduction of J' down to $J'/J \simeq 0.2$. Below this value, antiferromagnetic correlations grow weaker, a description of the ground state in terms of a Néel phase renormalized by quantum fluctuations becomes inadequate, and the finite-size spectra develop features that are not compatible with antiferromagnetic ordering. However, this phase does not appear to be connected to the kagome phase as well, as the low-energy spectra do not evolve with continuity for $J' \to 0$ to the kagome limit. In particular, for any nonzero value of J', the latter interaction sets the energy scale for the low-lying spin excitations, and a gapless triplet spectrum, destabilizing the kagome phase, is expected.

DOI: 10.1103/PhysRevB.69.224414 PACS number(s): 75.10.Jm, 75.40.Mg

I. INTRODUCTION

Geometrically frustrated antiferromagnets are the historical candidates for the realization of a *spin liquid* ground state. Indeed, the spin-half Heisenberg antiferromagnet on the triangular lattice was the first model to be proposed by Anderson and Fazekas[1,2] in 1973 as a system where geometric frustration and quantum fluctuations could prevent zero-temperature magnetic ordering in two dimensions, stabilizing instead a ground state with gapped spin excitations and exponentially decaying correlations. Since then, a good amount of work has been devoted to investigate the nature of the ground state of the triangular Heisenberg model[3–14] which remained an open question until quite recently. At present, however, there is a general consensus on the existence of long-range antiferromagnetic order following a 120° Néel pattern in the ground state of this model;[5,6,12,14] frustration and quantum fluctuations on the two-dimensional triangular lattice are not strong enough to stabilize a nonmagnetic ground state.

A more promising candidate for a disordered ground state can be obtained through a "dilution" of the triangular lattice, leading to the so-called *kagome* net (Fig. 1). In fact, on this geometry, due to the lower coordination ($z=4$ compared with $z=6$ in the triangular case), frustration is much stronger and even in the classical limit it gives rise to an infinite number of classical ground states, with ordered and disordered configurations degenerate in energy.[15–17] Due to the extensive entropy of the classical ground state, the so-called *order from disorder* mechanism—usually stabilizing, among degenerate manifolds, long-range ordered configurations—is much less effective than in other frustrated models. In particular, while harmonic fluctuations select planar configurations, they turn out to be completely insensitive to their degree of order, and only nonlinear effects eventually stabilize a classical ground state with Néel correlations with a $\sqrt{3}\times\sqrt{3}$ pattern (see Fig. 1). Whether such classical minimum energy configuration possesses true long-range order[15] or it is a critical point with power-law correlations[16,17] is still an open issue. In any case, due to the particularly delicate mechanism leading to the classical antiferromagnetic order, the latter is expected to be easily destabilized by quantum fluctuations.

The investigation of the quantum Heisenberg antiferromagnet on the kagome lattice has been capturing increasing attention[18–29] for some time now. Mainly on the basis of numerical work, evidence has accumulated supporting a spin-liquid ground state, even though a very peculiar one: this, in fact, would be characterized by a small gap ($\sim J/20$) to spin excitations, and by an exponentially large number of singlets contiguous to the ground state.[25–29] The classification of spin liquid of Type II has been recently proposed[28] to classify this particular behavior.

On the experimental side, the triangular geometry provides the scenario for interesting physical phenomena taking

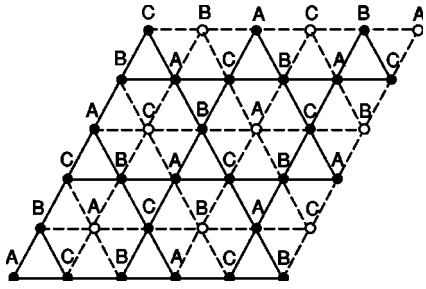

FIG. 1. The depleted triangular lattice. Filled and empty circles are the kagome and nonkagome sites; solid and dashes lines indicate J and J' bonds of the Hamiltonian (1). The letters A,B,C label the three different spin directions oriented 120° apart of the $\sqrt{3}\times\sqrt{3}$ classical Néel state.

place in the superconducting compounds $Na_xCoO_{2-y}H_2O$ (Ref. 31) and the organic materials $\kappa-(BEDT-TTF)_2X$, with X being I_3, $Cu[N(CN)_2]Br$ or $Cu(SCN)_2$[32]. Two spin-1/2 kagomelike materials have been also recently reported, the Volborthite $Cu_3V_2O_7(OH)_2\ 2H_2O$ Ref. 33 and the kagome-staircase compounds $Ni_3V_2O_8$ and $Co_3V_2O_8$.[34]

In the present work, we consider the spin-1/2 Heisenberg antiferromagnet on a lattice that interpolates between the triangular and the kagome ones. The Hamiltonian is

$$\hat{H} = J\sum_{\langle ij\rangle} \hat{\mathbf{S}}_i \cdot \hat{\mathbf{S}}_j + J' \sum_{\langle ij'\rangle} \hat{\mathbf{S}}_i \cdot \hat{\mathbf{S}}_{j'}, \tag{1}$$

where $\hat{\mathbf{S}}_i$ are spin-half operators, $\langle ij\rangle$ denotes nearest-neighbor bonds belonging to the kagome lattice, and $\langle ij'\rangle$ are the remaining bonds connecting kagome and nonkagome sites. A scheme is indicated in Fig. 1. In this way, $J'=J$ corresponds to the usual triangular lattice, while $J'=0$ defines the kagome one. Our aim is to start from the triangular limit and to investigate the stability of the ordered state as J'/J decreases. This is sensible because the classical Néel state on the triangular lattice is compatible with the expected $\sqrt{3}\times\sqrt{3}$ classical ordering on the kagome antiferromagnet. The first to study this model were Zeng and Elser,[22] who performed a spin-wave analysis and concluded that, for spin-1/2 particles, the ordered state could be stable for J' down to $J'/J \simeq 0.2$. Very recently, this model has been investigated with a coupled cluster treatment.[35] This technique is based on the three-sublattice structure characterizing the 120°-Néel order of the triangular lattice, which is found to break down very close to $J'=0$, indicating the instability of the magnetic ordered state very close to the kagome limit.

In this paper, we tackle this problem using variational approaches, and exact diagonalization of small clusters. In particular, in Sec. II, we employ the so-called fixed-node (FN) technique[30] in order to improve the accuracy of a wave function with long-range antiferromagnetic order previously introduced in the pure triangular case.[3,12] This technique, is usually used in the context of quantum Monte Carlo simulations as a method to approximate the Hamiltonians affected by sign-problem instabilities[30] and obtain exact ground-state properties of the corresponding "effective Hamiltonian," no longer affected by the sign problem. Here we use the FN method to define a variational state with long-range antiferromagnetic order, and we check its accuracy in describing the ground state of the model as J'/J is reduced through a direct comparison with exact diagonalization results on the 6×6 cluster. In order to detect any indication of a change in the nature of the ground state approaching the kagome limit, in Sec. III we analyze the structure of the low-energy spectra as a function of J'/J, using the exact diagonalization of the Hamiltonian on small clusters. Section IV is finally devoted to summary and conclusions.

II. VARIATIONAL APPROACHES

A fairly accurate representation of the ground state of the spin-1/2 Heisenberg antiferromagnet on the triangular lattice can be obtained starting from a 120° Néel ordered state and including Gaussian fluctuations by means of a Jastrow factor containing two-spin correlations[3,12]

$$|\psi_v\rangle = \hat{P}_0 \exp\left(\frac{1}{2}\sum_{i,j} v(i-j)\hat{S}_i^z\hat{S}_j^z\right)|N\rangle, \tag{2}$$

where $\hat{P}_0$ is the projector onto the $S^z=0$ subspace, $|N\rangle$ is the classical Néel state in the xy plane,

$$|N\rangle = \sum_x \exp\left[\frac{2\pi i}{3}\left(\sum_{i\in \mathrm{B}} S_i^z - \sum_{i\in \mathrm{C}} S_i^z\right)\right]|x\rangle, \tag{3}$$

and $|x\rangle$ is an Ising spin configuration specified by assigning the value of S_i^z for each site. On the square lattice case, the classical Néel state reproduces exactly the phases of the ground state of the Heisenberg Hamiltonian according to the Marshall theorem.[12] On the triangular lattice, instead, the exact phases of the ground state are unknown, and the classical part of the wave function (2) does not reproduces them accurately. However, as originally suggested by Huse and Elser,[3] a very accurate ansatz of the ground-state phases can be obtained by including three-spin correlation factors of the form:

$$T(x) = \exp\left(i\ \beta \sum_{\langle i,j,k\rangle} \gamma_{ijk} S_i^z S_j^z S_k^z\right), \tag{4}$$

defined by the coefficients $\gamma_{ijk}=0,\pm 1$, appropriately chosen so as to preserve the symmetries of the classical Néel state, and by the variational parameter β. In particular the sum in Eq. (4) runs over all distinct triplets of sites i,j,k where both i and k are nearest neighbors of j, and i and k are next-nearest neighbors to one another. The sign factor $\gamma_{ijk}=\gamma_{kji}=\pm 1$ is invariant under rigid translations and rotations in real space by an angle of 120° of the three-spin cluster i,j,k, but changes sign under rotations by 60°. The resulting wave function reads therefore:

$$|\psi_v\rangle = \hat{P}_0 \sum_x \Omega(x) \exp\left(\frac{1}{2}\sum_{i,j} v(i-j) S_i^z S_j^z\right)|x\rangle, \tag{5}$$

with the phase factor given by

$$\Omega(x) = T(x)\exp\left[\frac{2\pi i}{3}\left(\sum_{i\in \mathrm{B}} S_i^z - \sum_{i\in \mathrm{C}} S_i^z\right)\right]. \tag{6}$$

Since the Hamiltonian is real, a better variational wave function is defined by the real part of Eq. (5).

The two-body Jastrow potential in (5) contains in principle as many variational parameters as the independent distances on the lattice. However, the same level of accuracy can be obtained by optimizing separately the nearest-neighbor and next nearest-neighbor distances and adopting for the longer-range correlations an expression based on the consistency with linear spin-wave theory:[12]

$$v(r) = \frac{\eta_\infty}{N}\sum_{q\neq 0} e^{-iq\cdot r} v_q \tag{7}$$

with

TABLE I. Variational parameters and variational energies for the spin-wave wave function (5) for different values of the ratio J'/J on the $N=36$ cluster. The Lanczos exact values of the energy are also reported for comparison.

J'/J	β	η_1	η_1'	η_2	η_∞	E_v/J	E_0/J
0.1	0.20	−0.63	−0.58	0.055	1.00	−10.7687	−12.0799
0.2	0.20	−0.63	−0.58	0.055	1.00	−11.7299	−12.7120
0.3	0.20	−0.63	−0.58	0.055	1.00	−12.6911	−13.5026
0.4	0.20	−0.63	−0.58	0.055	1.00	−13.6522	−14.3708
0.6	0.20	−0.65	−0.62	0.055	1.00	−15.5730	−16.2287
0.8	0.23	−0.70	−0.69	0.055	1.00	−17.4873	−18.1754
1.0	0.23	−0.73	−0.73	0.055	1.00	−19.4239	−20.1734

$$v_q = 1 - \sqrt{\frac{1+2\gamma_k}{1-\gamma_k}}, \tag{8}$$

$\gamma_k = 2(\cos k_x + 2\cos k_x/2 \cos \sqrt{3}k_y/2)$ and η_∞ is a variational parameter. For the anisotropic triangular lattice (see Fig. 1) we have optimized separately the nearest-neighbor bonds connecting two kagome sites (η_1), and a kagome site and a nonkagome site (η_1'), as well as the next-nearest-neighbor bonds (η_2). As a result, the total number of variational parameters for the present variational wave function is 5. Their optimal values, and the corresponding variational energies, are reported for $N=36$ in Table I, for various values of J'/J.

The accuracy of the present long-range ordered wave function in the triangular lattice limit ($J'/J=1$) has been analyzed in detail in Refs. 12 and 13. In this limit the wave function is known to provide a qualitatively correct representation of the ground-state correlations.[3,12–14] In order to check the accuracy within a larger range of J'/J we have compared several variational properties with the exact ground-state values calculated by exact diagonalization on the largest cluster presently accessible, $N=36$. As shown in Fig. 2, for $0.4 \lesssim J'/J \leqslant 1$ both the accuracy on the ground-state energy and the overlap with the exact ground state, remain approximatively constant and equal to the values in the triangular limit ($J'/J=1$). In addition, the wave function (2) provides an accurate representation of the phases of the actual ground state up to $J'/J \simeq 0.2$, as it can be checked by measuring the average-sign

$$\langle s \rangle = \sum_x \mathrm{sgn}[\psi(x)\psi_0(x)]|\psi_0(x)|^2, \tag{9}$$

with $|\psi_0\rangle = \Sigma_x\, \psi(x)|x\rangle$ (Fig. 2). This remarkable feature is due to the presence of the triplet term (4), allowing us to adjust the phases in a nontrivial way, without changing the underlying Néel order. For instance, in the triangular limit the average sign (overlap) of the wave function is 0.733 (0.562) without the triplet term and 0.932 (0.779) with it.

Since the variational wave function (2) reproduces accurately the phases of the ground state its quality can be improved by adopting the FN scheme of Ref. 30. This allows one to obtain a new variational wave function, $|\psi_{\mathrm{FN}}\rangle$, defined as the ground state of the so-called FN effective Hamiltonian, whose matrix elements, $H^{\mathrm{eff}}_{x,x'}$, can be constructed starting from the original Hamiltonian and a variational guess on the ground-state phases given, in our case, by the wave function (5), $|\psi_v\rangle = \Sigma_x\, \psi_v(x)|x\rangle$:

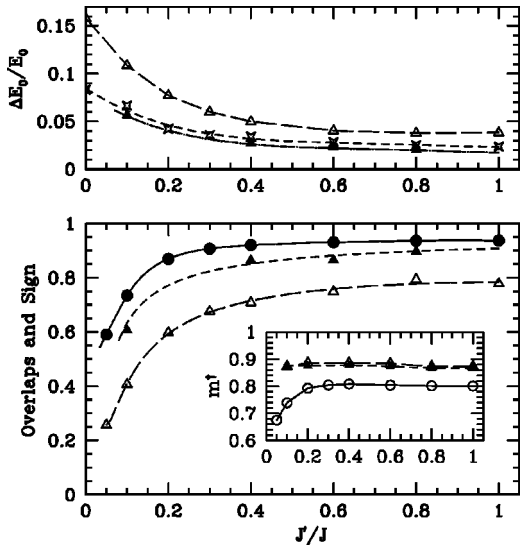

FIG. 2. Results on the $N=36$ cluster. Upper panel: Relative error on the ground-state energy, for the spin-wave (empty triangles) and FN (full triangles) wave functions. Stars refer to the accuracy of the upper bound on the energy given by the lowest eigenvalue of the FN Hamiltonian, E_0^{FN}. Lower panel: average sign of both the spin-wave and FN wave function (circles) and their overlap with the exact ground state (same symbols as above). Inset: antiferromagnetic order parameter. The circles are the exact ground-state values, while empty and full triangles correspond to the results obtained with spin wave and FN wave functions, respectively. Lines are guides for the eye.

$$H^{\mathrm{eff}}_{x',x} = \begin{cases} H_{x',x} & \text{if} \quad \overline{H}_{x',x} \leqslant 0 \\ 0 & \text{if} \quad \overline{H}_{x',x} > 0 \\ H_{x,x} + \mathcal{V}(x) & x = x' \end{cases} \tag{10}$$

where $\overline{H}_{x',x} = \psi_v(x')H_{x',x}/\psi_v(x)$, and

$$\mathcal{V}(x) = \sum_{\{\overline{H}_{x',x}>0,\, x'\neq x\}} \overline{H}_{x',x}. \tag{11}$$

Indicating with E_0^{FN} the ground-state energy of the FN Hamiltonian, with $E_v^{\mathrm{FN}} = \langle\psi_{\mathrm{FN}}|\hat{H}|\psi_{\mathrm{FN}}\rangle/\langle\psi_{\mathrm{FN}}|\psi_{\mathrm{FN}}\rangle$ and $E_v = \langle\psi_v|\hat{H}|\psi_v\rangle/\langle\psi_v|\psi_v\rangle$ the energy expectation values on $|\psi_{\mathrm{FN}}\rangle$ and $|\psi_v\rangle$, respectively, it is possible to show[30] that the following chain of inequalities holds:

$$E_v \geqslant E_0^{\mathrm{FN}} \geqslant E_v^{\mathrm{FN}} \geqslant E_0,$$

where E_0 is the ground-state energy of $\hat{H}$. Hence, the FN procedure is granted to produce a wave function with a better variational energy than $|\psi_v\rangle$. In addition, also the lowest eigenvalue of the FN Hamiltonian, E_0^{FN}, gives an upper bound of the ground-state energy better than the variational energy E_v. This is the quantity which is usually considered in the

quantum Monte Carlo application since it is the most directly accessible.

The FN Hamiltonian is explicitly defined in such a way that the matrix $\bar{H}^{\rm eff}_{x',x}=\mathrm{sgn}[\psi_v(x')]H^{\rm eff}_{x',x}\,\mathrm{sgn}[\psi_v(x)]$ has all negative off-diagonal matrix elements. By the Perron-Frobenius theorem, the amplitudes of the ground state of this matrix, $\bar{\psi}_{\rm FN}(x)$, have the same sign for all the configurations $|x\rangle$. This implies in turn that the FN ground state, $|\psi_{\rm FN}\rangle$, and the starting variational wave function, $|\psi_v\rangle$, have exactly the same phases. In fact, the amplitudes of the ground state of $H^{\rm eff}_{x',x}$, $\psi_{\rm FN}(x)$, are related to the amplitudes of the ground state of the transformed matrix $\bar{H}^{\rm eff}_{x',x}$, $\bar{\psi}_{\rm FN}(x)$, by the simple relation $\bar{\psi}_{\rm FN}(x)=\psi_{\rm FN}(x)\mathrm{sgn}[\psi_v(x)]$. For this reason, the FN wave function is expected to provide an accurate description of the ground state only when it is constructed with a good variational ansatz of the ground-state phases. In the present case for $0.2\lesssim J'/J\leqslant 1$.

In order to thoroughly check the accuracy of the FN wave function, we have exactly diagonalized with the Lanczos algorithm the FN Hamiltonian for several values of J'/J on the $N=36$ cluster. This has allowed us to calculate not only the FN energies but also the overlap of the FN wave function with the exact ground state. As shown in Fig. 2, both the FN upper bounds to the ground-state energy, $E_v^{\rm FN}$ and $E_0^{\rm FN}$, are sizably more accurate than the simple variational estimate E_v. In particular, the FN wave functions has a much higher overlap than $|\psi_v\rangle$, and its accuracy is almost constant and comparable to the one in the triangular limit down to values of J'/J as small as ~ 0.2.

We have finally compared the variational, FN, and exact estimates of the antiferromagnetic order parameter for a 120° Nèel order,

$$m^{\dagger 2}=36\frac{\mathcal{M}^2}{N(N+6)}, \tag{12}$$

where $\mathcal{M}^2$ is the sublattice magnetization squared.[6] Interestingly, by decreasing J'/J the exact ground-state order parameter remains approximatively constant down to $J'/J\simeq 0.2$ thus indicating a possible destabilization of the antiferromagnetic order only very close to the kagome limit. In addition, though the variational and FN estimates of the order parameter are approximatively 10% higher than the exact one the same degree of agreement is observed in all the range $0.2\lesssim J'/J\leqslant 1$. For the $N=36$ cluster, the FN wave function, based on the variational wave function (5), provides a good quantitative description of the exact ground state for $0.2\lesssim J'/J\leqslant 1$. In this range, the variational and the exact expectation values of antiferromagnetic order parameter remain constant and equal to their values in the triangular limit. Below $J'/J\simeq 0.2$, the exact value of the order parameter begins to decrease and the accuracy of the our Néel ordered wave function quickly degrades, indicating a change in the ground-state correlations only very close to the kagome limit.

In order to support further the stability of the antiferromagnetic phase for very small values of J'/J we have extended the variational and the FN calculations of the order parameter $m^\dagger$ to much larger sizes by using quantum Monte Carlo techniques.[36] As shown in Fig. 3, even at a value of $J'/J=0.2$, the lowest coupling ratio when the variational wave function is expected to be accurate (see Fig. 2), the order parameter $m^\dagger$ remains sizably larger than the triangular $J'/J=1$ case. This indicates that, as we increase the size at fixed ratio $J'/J<1$, the stability of the ordered phase, already evident in the exact diagonalization in the $N=36$ cluster (see Fig. 2), becomes more and more clear. We expect that this qualitative behavior, confirmed both by the exact diagonalization, and even more strongly by the variational and the FN approaches on larger sizes, is a genuine feature of the model, even though the quantitative results that we have obtained by quantum Monte Carlo may be affected by a sizable error. This feature may appear rather surprising, as the quantum fluctuations should increase for small J'/J and should tend to destabilize the ordered phase, as expected for instance within spin-wave theory.[18] However, the wave function that we have used is consistent with spin-wave theory in the large spin limit, and therefore, since also at the variational level the value of $m^\dagger$ increases, we conclude that the quantum fluctuations are not very accurately described within a method that is not controlled by the variational principle (the large spin limit), at least in the region of small J'/J.

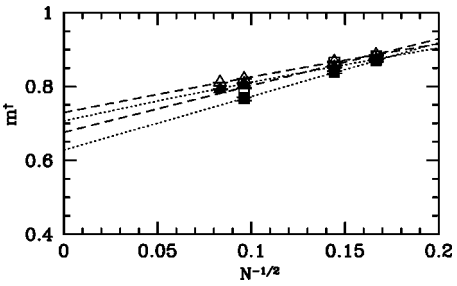

FIG. 3. Size scaling of the antiferromagnetic order parameter for the spin-wave (empty symbols and dashed lines), and the FN (full symbols and dotted line) wave functions: $J'/J=0.2$ (triangles), $J'/J=1.0$ (squares).

A similar size-scaling analysis can be carried out to estimate the ground-state energy per spin in the thermodynamic limit as illustrated in Fig. 4. The extrapolated energies are listed in Table II. Since the FN energy error is known exactly up to the 6×6 cluster, we can estimate the ground-state en-

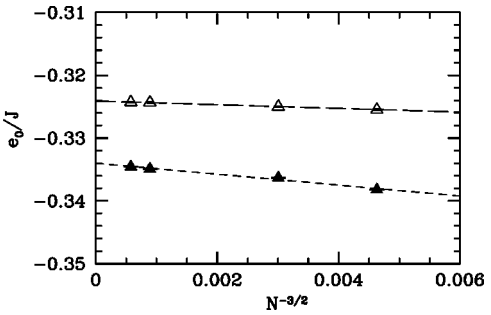

FIG. 4. Size scaling of the ground-state energy per spin for $J'/J=0.2$: Spin-wave wave function (empty triangles), FN (full triangles).

TABLE II. Ground-state energy per spin for different values of the J'/J ratio obtained with the spin-wave wave function (e_v), the FN technique (e_0^{FN}), and the estimated ground-state energy ($\tilde{e}_0^{\mathrm{FN}}$) obtained by assuming that the FN error in the energy is weakly size dependent (see text). The data for $J'/J=0$ are normalized to give the energy per spin on the kagome lattice. Uncertainties are of the order of one unit on the last digit. The coupled cluster method results, from Table I and Fig. 2 of Ref. 35, are also shown for comparison.

J'/J	0.0	0.2	0.4	0.6	0.8	1.0
e_v	−0.369	−0.324	−0.374	−0.425	−0.478	−0.532
e_0^{FN}	−0.392	−0.334	−0.381	−0.431	−0.482	−0.537
Ref. 35 ($m=6$)	−0.418	−0.346	−0.390	−0.438	−0.490	−0.543
$\tilde{e}_0^{\mathrm{FN}}$	−0.419	−0.349	−0.393	−0.443	−0.494	−0.550
Ref. 35 ($m\to\infty$)	−0.4252					−0.5505

ergy in the thermodynamic limit, by adding the 6×6 correction to the infinite-size FN estimate. The corresponding extrapolated values of the ground-state energy shown in the Table II represent reasonable benchmark values for this quantity (or at least good upper bounds), as the FN error is expected to increase weakly for larger sizes even for a good variational ansatz. This behavior has been verified up to 6×6, and is also very reasonable to expect in general for an approximate variational calculation.

In the triangular limit, $J'/J=1$, our estimated ground-state energy coincides with the corresponding one obtained with the coupled cluster method[35] by extrapolating in the size of the clusters ($m\to\infty$, with the notations of Ref. 35). This value is instead slightly lower than the extrapolated results based on small clusters ($N\leqslant 36$) obtained in Ref. 6, giving $e_0=-0.5445$. A good agreement between the coupled cluster for $m=6$ and the FN method is also seen for values of J'/J down to 0.2 (Table II). Furthermore, our extrapolated energies, based on the error for the 6 cluster and the FN energy, remain lower than the $m=6$ coupled cluster result by a similar amount, suggesting that our variational approach remains accurate enough also in this region (unfortunately the extrapolations $m\to\infty$ are not given in Ref. 35 for $0<J'/J<1$). Instead in the kagome limit our variational ansatz should be clearly less accurate, as the ground state is believed to be a spin liquid with no magnetic order in the thermodynamic limit, i.e., qualitatively different from our initial variational guess given by Eq. (2). This may explain why in this case our energy estimate is slightly higher than the $m\to\infty$ coupled cluster result. We note, however, that our values reported in Table II represent in general reasonable upper bounds for the energy, as they are obtained by a rigorous variational method such as the FN one.

III. LOW-ENERGY EXCITATIONS

An effective method to investigate the possibility of magnetic order in spin systems is to analyze the structure of the spectrum of finite-size samples, following the strategy of Refs. 5, 6, and 25. The tendency toward antiferromagnetic order in the thermodynamic limit manifests itself in finite-size clusters through the fact that the spin excitations with the lowest energies can be described by the effective Hamiltonian of a "quantum top." Within such a description, the energy of the lowest levels in the different subspaces labeled by total spin S, can be approximated by,

$$E_N(S)-E_N(0)=\frac{S(S+1)}{2I_N}, \tag{13}$$

where I_N is the inertia of the top, which is an extensive quantity. Hence, the plots of the lowest energy levels as functions of $S(S+1)$, have the appearance of a "Pisa tower" with a slope that decreases as N increases. An important property of the states of the "Pisa tower" (indicated in Ref. 6 *quasidegenerate joint states*) is that they belong to irreducible representations of the point group that are compatible with the symmetry of the ordered state. In the case of the $\sqrt{3}\times\sqrt{3}$ order, these are the representations labeled as $\Gamma_1,\Gamma_2,\Gamma_3$ of the C_{3v} group, which correspond to $[\mathbf{k}=0,\mathcal{R}_\pi\Psi=\Psi,\mathcal{R}_{2\pi/3}\Psi=\Psi,\sigma_x\Psi=\Psi]$; $[\mathbf{k}=0,\mathcal{R}_\pi\Psi=-\Psi,\mathcal{R}_{2\pi/3}\Psi=\Psi,\sigma_x\Psi=\Psi]$; $[\mathbf{k}=\mathbf{Q},\mathcal{R}_\pi\Psi=\Psi,\mathcal{R}_{2\pi/3}\Psi=\Psi,\sigma_x\Psi=\Psi]$, respectively. We have followed the same notation of Refs. 5, 6, and 25, $\mathcal{R}_\phi$ denoting a rotation of ϕ,σ_x, a reflection with respect to a mirror plane with the normal pointing along x, and being $\mathbf{Q}=(2\pi/3,-2\pi/3)$, the corner of the Brillouin zone of the kagome lattice.

There are not so many finite periodic clusters, which can be exactly diagonalized and that interpolate between the triangular and kagome lattices without frustrating the antiferromagnetic order. The smallest ones are $N=12$ and $N=36$, which evolve, respectively, toward $N=9$ and $N=27$ at the pure kagome limit ($J'=0$). The unit cell of the interpolating lattice contains 2×2 unit cells of the pure triangular lattice, implying a reduction of the translation operations of the periodic cluster of a factor 4 with respect to the number of translations at the pure triangular limit. This implies a much bigger Hilbert space to be dealt with in the numerical procedure. In concreteness, even exploiting all the available symmetries, the number of states is 42035724 for $N=36$ spins. In this cluster, a complete study of several excited states within different spin sectors for several values of J' is prohibitive from the computational point of view, while the $N=12$ cluster maybe too small. We have, therefore, included in the analysis the clusters with $N=16$ and $N=28$ sites (which evolve toward kagome clusters with $N=12$ and $N=21$, respectively), by introducing twisted boundary conditions as explained in Refs. 6 and 25. The latter are equivalent to

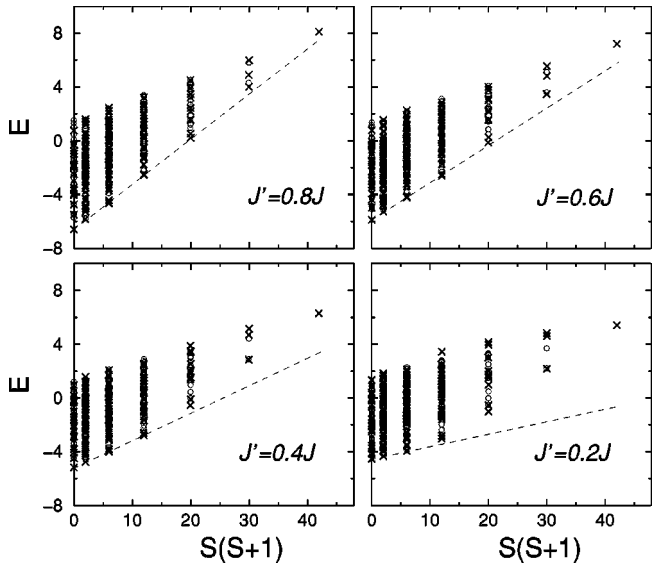

FIG. 5. Energy spectra as functions of $S(S+1)$ for a cluster with $N=12$ spins, periodic boundary conditions, and $J'/J=0.8$, 0.6, 0.4, 0.2 (left to right and top to bottom). The crosses (circles) indicate energy levels belonging to symmetry representations compatible (incompatible) with the $\sqrt{3}\times\sqrt{3}$ magnetic order.

rotate the local frame in $(\pm 2\pi/3, \mp 2\pi/3)$ at each translation along a unitary lattice vector. This procedure restores the otherwise frustrated antiferromagnetic order in the x,y spin plane but obviously breaks the spin-rotational symmetry as well as some symmetry operations of the point group. For this reason, in this case, a law like that expressed in (13), with the replacement $S(S+1)\rightarrow S_z^2$, should be obeyed by the quasi degenerate joint states, as the total S^z along the z axis, cannot couple with the remaining total spin components in the clusters with twisted boundary conditions. Results are shown in Figs. 5–7 for $N=12$, 16, and 28, respectively. Figures 5 and 6 show the full spectra, obtained by diagonalizing all the blocks of the Hamiltonian matrix. In the case of $N=28$ (Fig. 7), we have not diagonalized the full Hamiltonian

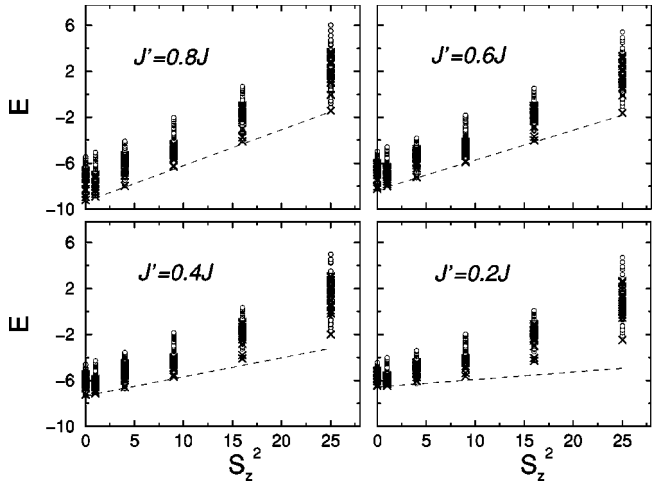

FIG. 6. Energy spectra as functions of S_z^2 for a cluster with $N=16$ spins and twisted boundary conditions. Details are the same as in Fig. 5.

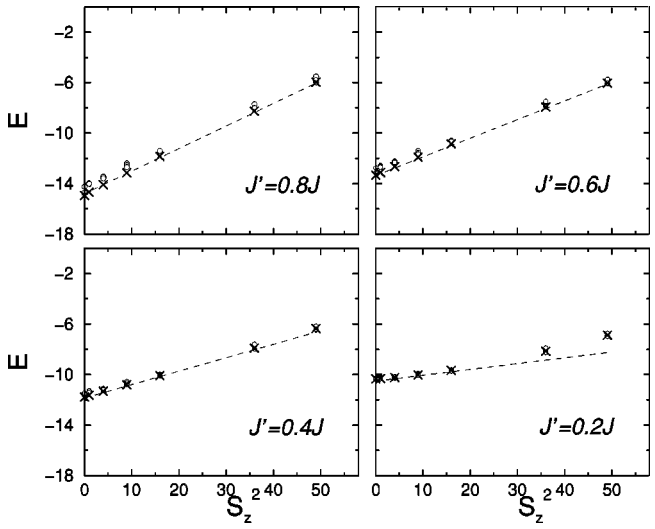

FIG. 7. Lowest energy levels within the different S_z^2 subspaces for $N=28$ and twisted boundary conditions. Details are the same as in Fig. 5.

but obtained the lowest eigenvalues within all the subspaces using the Lanczos algorithm.

We have plotted the states with symmetries compatible (noncompatible) with the antiferromagnetic $\sqrt{3}\times\sqrt{3}$ order with crosses (circles). The first striking feature is the fact that only a subset of the states forming the "Pisa tower" in the triangular limit remains aligned as J'/J decrease. Those states build up, so to say, a "small Pisa tower," whose slope decreases with J'.

In order to analyze in more detail the behavior of the states along the "small Pisa tower" we show zooms of the low-energy and low-spin sector of the spectra for the $N=12$, and $N=28$ clusters in Figs. 8 and 9, respectively. In the case of $N=12$, shown in Fig. 8, this small set contains levels that belong to representations compatible with the $\sqrt{3}\times\sqrt{3}$ order

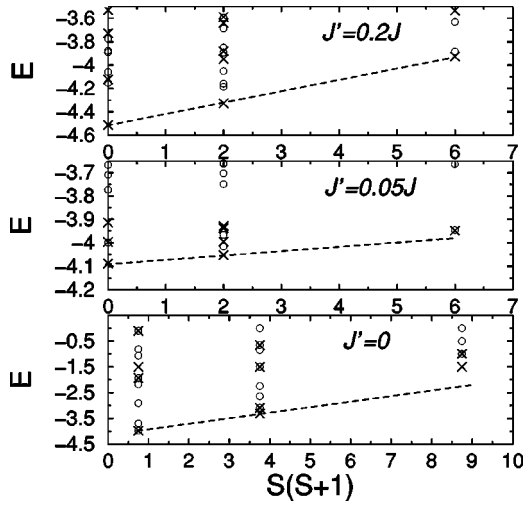

FIG. 8. Detail of the low-lying energy levels close to the kagome limit for a cluster with $N=12$ spins and periodic boundary conditions. The lower panel shows the behavior of the low energy levels at the kagome limit in a cluster with $N=9$ sites. Details are the same as in Fig. 5.

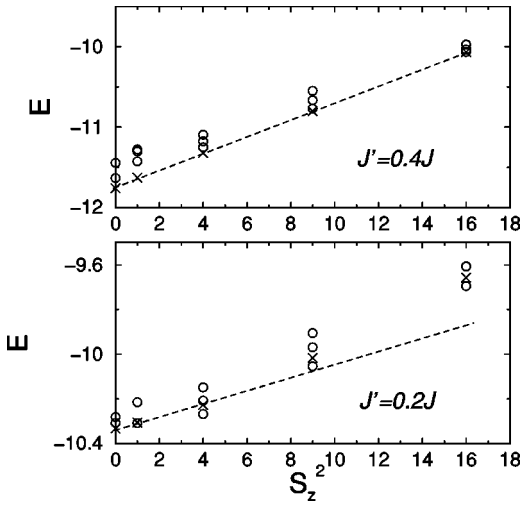

FIG. 9. Detail of the low-lying energy levels close to the kagome limit for a cluster with $N=28$ spins and twisted boundary conditions. Details are the same as in Fig. 5.

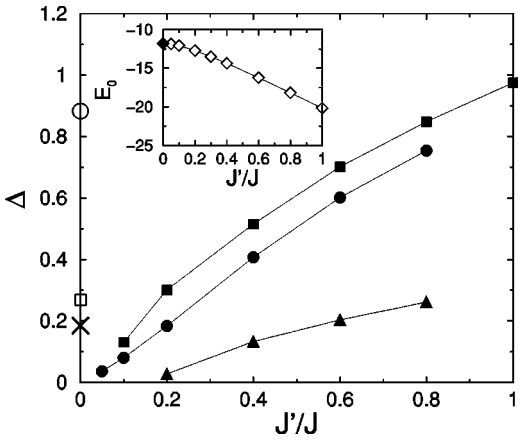

FIG. 10. Gap to the lowest excitation with $\Delta S_z=1$ for $N=12$ (circles), $N=28$ (triangles), and (in the Γ_1 representation) $N=36$ (squares). The open circle and square at $J'=0$ indicate the value of the spin gap for the $N=9$ and $N=27$ kagome cluster (corresponding to the $N=12$ and $N=36$ depleted triangular clusters). The cross at $J'=0$ corresponds to a kagome cluster with $N=36$. Inset: The ground-state energy as function of J' (open diamonds). The filled diamond indicates the ground-state energy of the kagome cluster with $N=27$ spins.

and they remain aligned within all the range $0.1 \leqslant J'/J \leqslant 1$. Signatures of departure from that behavior are observed for very low $J'/J=0.05$, where the lowest level with $S=2$ deviates from the line of the "small Pisa tower" while a state with a symmetry not compatible with the antiferromagnetic order becomes quasidegenerate with it. In Fig. 8 the data for the related $N=9$ kagome lattice are also shown. In that case, a similar deviation of the state with $S=5/2$ from the line connecting the lowest levels in the $S=1/2$ and $S=3/2$ sectors is observed but within a scale which is an order of magnitude larger in the energy axis. Another contrasting feature that comes from the comparison between $J'=0$ and $J' \neq 0$ is that in the pure kagome limit, there are two states with $S=1/2$ (one of them belonging to the manifold of the degenerate ground state) whose symmetries are not compatible with the $\sqrt{3}\times\sqrt{3}$ order that have energies within the spin gap. Instead for $J'/J=0.05$ the spin gap is clean from such states. In addition, the gap to the lowest excitation with $\Delta S=1$ does not evolve with continuity for $J'/J \to 0$ to the corresponding gap in the kagome limit (see also Fig. 10).

Similar remarks apply to the 16- and 28-sites clusters shown in Figs. 6 and 7. In these cases, see e.g., Fig. 9, the "small Pisa Tower" contains a larger number of states but the deviation from a perfect alignment is observed already at $J'/J \leqslant 0.2$, where states within subspaces not compatible with the $\sqrt{3}\times\sqrt{3}$ order appear at low energies. In particular, for $S_z=1$ one of those states is almost degenerate with the one belonging to the Pisa tower while for $S_z=2$ it is well below it. As in the $N=12$ cluster, also for $N=16$ and 28 the gap to the first spin excitation monotonically decreases with J' (Fig. 10).

To complete the analysis, we have computed the ground-state energy (E_0) and the lowest eigenvalue in the subspace with $S=1$ within the representation Γ_1 of C_{3v} ($E_{S=1,\Gamma_1}$), in the periodic lattice with $N=36$ sites. The latter does not actually correspond to the lowest energy $S=1$ excitation in the pure triangular limit, which is in the subspace corresponding to Γ_2. In any case, the energy difference $\Delta=E_{S=1,\Gamma_1}-E_0$ is, in general, an upper bound for the spin gap of the cluster in all the range $0<J'/J\leqslant 1$. The behavior of Δ as a function of J' is shown in Fig. 10. As in the clusters previously considered, the gap decreases rapidly as J' decreases, and, in particular, it does not evolve continuously for $J' \to 0$ towards the value of the corresponding kagome lattice ($N=27$, indicated with an open square in Fig. 10). Instead, it tends to a value which is even smaller than the magnitude of the spin gap for the $N=36$ kagome lattice (indicated by a cross in the same figure). This is in contrast with the behavior exhibited by the ground-state energy, which evolves smoothly toward the value of the $N=27$ kagome lattice (see the inset of Fig. 10).

The behavior of the spin gap and the spectra strongly suggests the closing of the spin-gap in the thermodynamic limit within the whole range of $0<J'/J\leqslant 1$. In fact, such gap is known to close in the thermodynamic limit at the triangular point ($J'/J=1$) (Refs. 5, 6, and 12) and it decreases systematically by decreasing J' in all the cluster considered as the low-energy scale for the lowest-spin excitations is set by J', i.e., by the states of the "small Pisa tower." This can be understood in a simple uncorrelated framework where for $J'<J$ the lowest spin-excitations are clearly obtained through a spin-flip on a nonkagome site, with an energy cost $6J'$, compared to a cost $4J+2J'$ for a spin-flip on a kagome site. As the number of nonkagome spins is just a fraction of the total number of sites, on a finite cluster such a mechanism would apply only to the lowest spin excitations: hence the reduction of the number of states belonging to the "Pisa tower" with respect to the triangular case.

This simple picture immediately suggests that the nature of the spin excitations is intrinsically different for finite J' and in the pure kagome limit. In the latter case, in fact, the spins on the nonkagome sites do not belong to the Hilbert space of the model and such low-energy spin excitations are not possible. For this reason by turning on the J', the spin

gap has a finite discontinuity and it is reasonable to expect the model to be unstable under the perturbation introduced by J' bonds. This is also confirmed by the analysis of the low-energy excitations for small values of J'/J (see Fig. 8).

One step further in the analysis of the nature of the ground state leads to the question whether or not the latter remains ordered down to the kagome limit. The structure of the spectra of the small $N=12$ cluster indicates that could well be the case, while those of $N=16$ and $N=28$ suggests some change in the nature of the ground state around $J'/J \sim 0.2$. It is worth recalling, however, that the results for the two latter clusters have been obtained by using twisted boundary conditions which could lead to weaker signatures of ordering. On the other hand, in two dimensions, it seems difficult to conceal the possibility of the closing of the spin gap with the absence of some kind of magnetic order. A simple geometrical analysis reveals that the nonkagome spins, which we have already identified as the responsible of the lowest-energy excitations, form themselves a triangular lattice with a cell parameter twice the size of the one of the usual triangular lattice. Therefore, a possible scenario for the evolution of the ground state as J' decreases could be that at some point a crossover takes place from a magnetic order in the usual $\sqrt{3}\times\sqrt{3}$ pattern to a magnetic order with a similar pattern but in the triangular lattice of the nonkagome spins. Both kinds of order are commensurate and the ground state could undergo a smooth evolution from one to the other.

IV. SUMMARY AND CONCLUSIONS

We have investigated the low energy properties of a $J'-J$ triangular lattice that interpolates between the usual triangular $(J'/J=1)$ and kagome $(J'=0)$ lattices. To this end, we have used a variational approach based on a FN wave function accurately describing the ground state in the triangular $(J'/J=1)$ limit, and exact diagonalization techniques.

We have analyzed the quality of the approximation to the exact ground state, provided by the FN technique in a periodic cluster with $N=36$ sites and then extended the calculation up to $N=144$ sites by using quantum Monte Carlo calculations. We have found that such a wave function, describing a state with a $\sqrt{3}\times\sqrt{3}$ Néel ordered phase, is very close to the exact one for $0.2 \lesssim J'/J \leqslant 1$ and that in this range its accuracy is almost independent of the J'/J ratio. Consistently, the ground-state expectation value of the antiferromagnetic order parameter remains approximately constant down to $J'/J \simeq 0.2$. Below this value the order parameter is suppressed and the quality of the FN wave function degrades, suggesting a change in the nature of the ground-state. This is also confirmed by the analysis of the low-energy spectra on small clusters, showing some signatures of instability of Néel ordering for $J'/J \lesssim 0.2$. However, at the same time, such analysis also indicates quite clearly that the low-energy scale for spin excitations is set by J' and that in particular the spin-gap has a finite discontinuity at $J'/J=0$, the triplet excitations being gapless for any nonzero value of J'/J. This would imply that the kagome disordered phase is unstable against a slight perturbation tending to restore the $z=6$ coordination number of the triangular lattice. A possible scenario is that within the large amount of singlets that are quasidegenerate with the ground state in the kagome clusters, the one corresponding to the $\sqrt{3}\times\sqrt{3}$ state is favored by some kick produced by J'.

Our results are in disagreement with the predictions of the spin-wave theory of Ref. 18, indicating a progressive reduction of the antiferromagnetic ordering for $J'/J<1$ and a complete melting of the $\sqrt{3}\times\sqrt{3}$ order for $(J'/J)_c \simeq 0.2$. Instead, our conclusions are closer to those of the recent coupled cluster treatment of Farnell *et al.*[35] providing evidence for instability of the antiferromagnetic order very close or possibly at the kagome point $((J'/J)_c = 0.0 \pm 0.1)$, and the existence for small J'/J of a regime whose correlations are very different to those of the triangular antiferromagnet. Further investigations are necessary to clarify the nature of this regime.

ACKNOWLEDGMENTS

L. A. thanks Professor Fulde for his hospitality as well as the Alexander-von-Humboldt Stiftung and CONICET, Argentina for the support. This work was partially supported by INFM-PRA MALODI, and by NSF under Grant No. DMR02-11166 (L.C.).

*Permanent address: Departamento de Física, Universidad de Buenos Aires, Ciudad Universitaria Pabellón I, (1428) Buenos Aires, Argentina.

[1] P. W. Anderson, Mater. Res. Bull. **8**, 153 (1973).
[2] P. Fazekas and P. W. Anderson, Philos. Mag. **30**, 423 (1974).
[3] D. A. Huse and V. Elser, Phys. Rev. Lett. **60**, 2531 (1988).
[4] R. Singh and D. Huse, Phys. Rev. Lett. **68**, 1766 (1992).
[5] B. Bernu, P. Lecheminant, C. Lhuillier, and L. Pierre, Phys. Rev. Lett. **69**, 2590 (1992).
[6] B. Bernu, P. Lecheminant, C. Lhuillier, and L. Pierre, Phys. Rev. B **50**, 10048 (1994).
[7] P. W. Leung and K. J. Runge, Phys. Rev. B **47**, 5861 (1993).
[8] K. Yang, L. K. Warman, and S. M. Girvin, Phys. Rev. Lett. **70**, 2641 (1993).
[9] P. Sindzingre, P. Lecheminant, and C. Lhuillier, Phys. Rev. B **50**, 3108 (1994).
[10] T. Jolicoeur, E. Dagotto, E. Gagliano, and S. Bacci, Phys. Rev. B **42**, 4800 (1990).
[11] P. Azaria, B. Delamonte, and D. Mouhanna, Phys. Rev. Lett. **70**, 2483 (1993).
[12] L. Capriotti, A. E. Trumper, and S. Sorella, Phys. Rev. Lett. **82**, 3899 (1999); A. E. Trumper, L. Capriotti, and S. Sorella, Phys. Rev. B **61**, 11529 (2000); L. Capriotti, Int. J. Mod. Phys. B **15**, 1799 (2001).
[13] L. Capriotti, Ph.D. thesis, SISSA, Trieste, Italy, 2000.
[14] M. Boninsegni, Phys. Rev. B **52**, 15304 (1995).

[15] D. A. Huse and A. D. Rutenberg, Phys. Rev. B **45**, 7536 (1992).
[16] J. T. Chalker, P. C. W. Holdsworth, and E. F. Shender, Phys. Rev. Lett. **68**, 855 (1992).
[17] J. N. Reimers and A. J. Berlinsky, Phys. Rev. B **48**, 9539 (1993).
[18] C. Zeng and V. Elser, Phys. Rev. B **42**, 8436 (1990).
[19] J. T. Chalker and J. F. G. Eastmond, Phys. Rev. B **46**, 14 201 (1992).
[20] P. W. Leung and V. Elser, Phys. Rev. B **47**, 5459 (1993).
[21] N. Elstner and A. P. Young, Phys. Rev. B **50**, 6871 (1994).
[22] C. Zeng and V. Elser, Phys. Rev. B **51**, 8318 (1995).
[23] A. Chubukov, Phys. Rev. Lett. **69**, 832 (1992).
[24] L. O. Manuel, A. E. Trumper, C. J. Gazza, and H. A. Ceccatto, Phys. Rev. B **50**, 1313 (1994).
[25] P. Lecheminant, B. Bernu, C. Lhuillier, L. Pierre, and P. Sindzingre, Phys. Rev. B **56**, 2521 (1997).
[26] C. Waldtmann, H.-U. Everts, B. Bernu, C. Lhuillier, P. Sindzingre, P. Lecheminant, and L. Pierre, Eur. Phys. J. B **2**, 501 (1998).
[27] M. Mambrini and F. Mila, Eur. Phys. J. B **17**, 651 (2000).
[28] C. Lhuillier and P. Sindzingre, *Quantum Properties of Low-Dimensional Antiferromagnets*, edited by Yoshitami Ajiro and Jean-Paul Boucher (Kyushu University Press, Tokyo, 2002), p. 111.
[29] G. Misguich and C. Lhuillier, cond-mat/0310405 (unpublished).
[30] D. F. B. ten Haaf, H. J. M. van Bemmel, D. F. B. ten Haaf, J. M. J. van Leeuwen, W. van Saarloos, and D. M. Ceperley, Phys. Rev. B **51**, 13 039 (1995); S. Sorella and L. Capriotti, Phys. Rev. B **61**, 2599 (2000).
[31] K. Takada *et al.*, Nature (London) **422**, 53 (2003).
[32] R. H. McKenzie, Science **298**, 820 (1997).
[33] Z. Hiroi, M. Hanawa, N. Kobayashi, M. Nohara, H. Takagi, Y. Kato, and M. Takigawa, J. Phys. Soc. Jpn. **70**, 3377 (2001).
[34] N. Rogado, G. Lawes, D. A. Huse, A. P. Ramirez, and R. J. Cava, Solid State Commun. **124**, 229 (2002).
[35] D. J. J. Farnell, R. F. Bishop, and K. A. Gernoth, Phys. Rev. B **63**, 220402 (2001).
[36] M. Calandra and S. Sorella, Phys. Rev. B **57**, 11446 (1998).